22 September 1995

ELSEVIER

Chemical Physics Letters 243 (1995) 519–525

CHEMICAL PHYSICS LETTERS

Kinetics of the FNO + HO_2 reaction

M. Matti Maricq, Joseph J. Szente

Research Laboratory, Ford Motor Company, P.O. Box 2053, Drop 3083 Dearborn, MI 48121, USA

Received 28 April 1995; in final form 25 July 1995

Abstract

The reaction between FNO and HO_2 constitutes the propagation step in a chain reaction converting H_2 and F_2 into HF. Time resolved UV spectroscopy reveals that NO forms simultaneously with HO_2 disappearance indicating that the formation of $HF + NO + O_2$ is the major product channel. The measured rate constant for this reaction is $k_4 = (2.7^{+2.8}_{-1.3}) \times 10^{-13} e^{(742 \pm 190)/T}$ cm^3 s^{-1} over the temperature range 223–327 K and at a total pressure of 550–700 Torr. Analogous experiments indicate that the FNO + CH_3O_2 reaction proceeds with a rate constant $k < 5 \times 10^{-14}$ cm^3 s^{-1} at 295 K.

1. Introduction

Concern over the deleterious effects of chlorofluorocarbon compounds (CFCs) on the ozone layer has led to a phaseout of their use and to the introduction of a variety of replacement compounds. For many applications the materials of choice are the hydrochlorofluorocarbon (HCFC) and hydrofluorocarbon (HFC) compounds and this has led to a vigorous scientific study of their possible effects on the atmosphere. By the fact that they contain hydrogen, the HCFCs and HFCs are susceptible to OH attack, which initiates a series of degradation reactions. Because these compounds contain fluorine their chemistry is often quite different from that of the analogous non-halogenated hydrocarbons.

The first few steps in the degradation process, namely hydrogen abstraction by OH, O_2 addition to from a peroxy radical, and the subsequent reaction with NO to generate an alkoxy radical, are essentially the same for halogenated and non-halogenated alkanes. The subsequent chemistry, however, is quite different, particularly for compounds containing CF_3 or CF_2 groups. Such compounds release CF_3O or CF_2O, the latter of which, after photolysis in the stratosphere, leads to FC(O)O formation [1]. It had been speculated that CF_3O and FC(O)O could participate in ozone depletion cycles analogous to the one by which chlorine atoms destroy ozone [2,3]. Subsequent research has shown that the chain propagation steps are slow compared to termination reactions involving NO [4–7]. Since both CF_3O and FC(O)O react with NO to form FNO, it is of interest to examine the atmospheric fate of this species.

A preliminary discussion of the FNO + HO_2 reaction was given in a previous paper [8] on the atmospheric chemistry of FNO. There an upper limit of 3×10^{-12} cm^3 s^{-1} was reported for the rate constant along with upper limits for the reactions of FNO with O_3, $O(^3P)$, and HCl. The more detailed study presented here allows us to report temperature dependent rate constants for the FNO + HO_2 reaction. The results show that this reaction is competitive with photolysis for the removal of FNO. The HO_2 reaction represents a direct sink for FNO, converting it to HF, and it recycles the NO used in

SSDI 0009-2614(95)00882-9

the CF_3O and FC(O)O terminations reactions. Photolysis, in contrast, releases F atoms, which either reform FNO or are lost by reactions with water vapor and hydrocarbons. The study of the title reaction is made both more difficult and more interesting by the existence of a chain reaction whereby FNO catalyzes the conversion of H_2 and F_2 into HF, even in the presence of O_2. The relevant chemistry is discussed and the rate constants are reported in Section 3 following a brief description of the experimental procedure. Section 4 discusses the impact of the reaction on the stratospheric fluorine cycle.

2. Experimental

Measurements of the $FNO + HO_2$ reaction were made using a flash photolysis/time resolved UV spectrometer that has been previously described [9]. The apparatus consists of a 3.2 cm diameter by 51 cm long thermostatically jacketed reaction vessel through which passes longitudinally a photolysis pulse created by an excimer laser. The reaction mixture was probed by broadband UV light from a deuterium lamp that counterpropagates the cell, is dispersed by a monochromator, and impinges a gated diode array detector.

FNO was formed continuously via the reaction

$$F_2 + NO \rightarrow F + FNO, \quad (1)$$

by premixing an excess of F_2 with the desired amount of NO. Of the remaining F_2, which entered the reaction cell with H_2, O_2, and N_2, a small fraction was photolyzed by a ≈ 400 mJ, 351 nm pulse from an XeF excimer laser generating about 6×10^{14} cm^{-3} fluorine atoms. These react rapidly with H_2 molecules,

$$F + H_2 \rightarrow H + HF, \quad (2)$$

to produce hydrogen atoms. The addition of molecular oxygen,

$$H + O_2 + M \rightarrow HO_2 + M, \quad (3)$$

subsequently yields the desired transient population of HO_2.

Progress of the reaction was monitored by time resolved UV spectroscopy. Spectra recorded at various delay times were fit to linear combinations,

$$\mathrm{Abs}(\lambda, t) = \sigma_{HO_2}(\lambda)[HO_2](t)l + \sigma_{NO}(\lambda)[NO](t)l + \sigma_{O_3}(\lambda)[O_3](t)l,$$

of reference spectra for HO_2, NO, and O_3 to determine the contributions that each species makes to the total absorbance [1]. The time versus concentration profiles determined in this manner were fit to predictions of the reaction model discussed below to determine the $FNO + HO_2$ reaction rate constant.

Reagent gases were obtained from Matheson and Michigan Air Gas at purities of $> 99\%$ and were used without further purification. Their flows were regulated by Tylan flow controllers and their concentrations measured by timing their flows into a fixed volume. The cell temperature was controlled by a Neslab ULT-80dd recirculating chiller and the gases, except for F_2 and NO, were precooled/preheated to the set temperature. The temperature of the gas mixture was measured by thermocouples in the gas stream at the entrance and exit of the cell. Total pressure was likewise monitored at the cell entrance and exit by capacitance manometers.

3. Results

3.1. $FNO + HO_2$

One of the first observations that one makes upon adding H_2 to a $F_2/NO/O_2/N_2$ gas mixture is a temperature rise of the mixture. This rise is exacerbated by increasing the concentrations of H_2 or NO, by decreasing O_2 or the total pressure and by increasing the initial temperature. If, in addition, the gas mixture is exposed to pulses of 351 nm radiation the temperature rises further. The temperature rise

[1] The reference spectrum for HO_2 is from Ref. [10], the spectrum for O_3 is from Ref. [11] and the spectrum of NO is unpublished.

can be explained by postulating the following chain reaction:

chain initiation steps:

$$FNO + H_2 \rightarrow HNO + HF,$$

$$\Delta H = -25.5\,\text{kcal/mol}\ ^{2},$$

$$HNO + F_2 \rightarrow F + HF + NO,$$

$$\Delta H = -48.5\,\text{kcal/mol},$$

chain propagation steps: reactions (2) and (3) followed by

$$FNO + HO_2 \rightarrow HF + NO + O_2,$$

$$H = -31\,\text{kcal/mol}, \qquad (4)$$

and reaction (1);

net:

$$H_2 + F_2 \rightarrow 2HF.$$

In addition to these, Table 1 lists secondary reactions, in particular chain termination steps, that are involved in the chain mechanism. The additional initiation step of F_2 photolysis explains the enhanced temperature rise observed upon irradiation of the reaction mixture. Note that the role of oxygen in this chain reaction differs considerably from its role in the more typical Cl_2/hydrocarbon chains. In the latter case, O_2 addition converts alkyl radicals into peroxy radicals and, thereby, acts as a chain termination step. This is not the case here, since the peroxy radical that is formed is intimately involved in chain propagation.

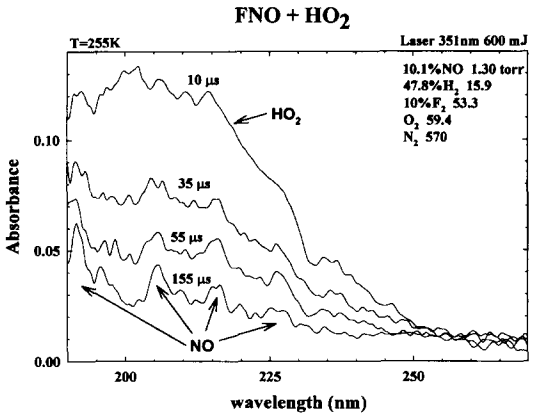

Fig. 1. Time resolved spectra of the reaction mixture following photolysis of a $F_2/NO/H_2/O_2/N_2$ gas mixture. Note the loss of HO_2 absorbance and the appearance of features due to NO. The small broad feature at about 250 nm is due to O_3.

Fig. 1 presents time resolved UV spectra of the reaction mixture following its photolysis. They show a broad initial absorbance centered at about 200 nm, and attributed to HO_2, that decays on the time scale of 100 μs. Closer examination, however, reveals the appearance of three narrower absorption features, at 205, 216, and 227 nm, that increase as the HO_2 decreases. Furthermore there is a broad and weak feature that arises at about 250 nm. The three sharp

[2] Heats of formation from Ref. [11].

Table 1
$FNO + HO_2$ reaction mechanism

Reaction [a]	Rate constant [b]
1. $F_2 + NO \rightarrow F + FNO$	$k = 7 \times 10^{-13}\, e^{-1150/T}\ cm^3\ s^{-1}$ [12]
2. $F + H_2 \rightarrow H + HF$	$k = 1.7 \times 10^{-10}\, e^{-550/T}\ cm^3\ s^{-1}$ [12]
3. $H + O_2 + M \rightarrow HO_2 + M$	$k = 5.7 \times 10^{-32}\, (T/300)^{-1.6}\ cm^6\ s^{-1}$
4. $FNO + HO_2 \rightarrow HF + NO + O_2$	$k = 2.7 \times 10^{-13}\, e^{742/T}\ cm^3\ s^{-1}$ [c]
5. $HO_2 + NO \rightarrow NO_2 + OH$	$k = 3.7 \times 10^{-12}\, e^{250/T}\ cm^3\ s^{-1}$
6. $F + O_2 + M \rightarrow FO_2 + M$	$k = 4.4 \times 10^{-33}\, (T/300)^{-1.2}\ cm^6\ s^{-1}$
7. $HO_2 + HO_2 \rightarrow H_2O_2 + O_2$	$k = 2.3 \times 10^{-13} e^{600/T} + 1.7 \times 10^{-33}\, e^{1000/T}\, P_{tot}\ cm^3\ s^{-1}$
$H + HO_2 \rightarrow$ products	$k = 8.1 \times 10^{-11}\ cm^3\ s^{-1}$
$FO_2 + NO \rightarrow FNO + O_2$	$k = 7.5 \times 10^{-12}\, e^{-688/T}\ cm^3\ s^{-1}$ [13]
$H + F_2 \rightarrow H + HF$	$k = 1.4 \times 10^{-11}\, (T/298)^{1.4}\, e^{-667/T}\ cm^3\ s^{-1}$ [12]
$H + FNO \rightarrow HF + NO$	$k = (0\text{–}4) \times 10^{-11}\ cm^3\ s^{-1}$
$NO_2 + HO_2 \rightarrow HO_2NO_2$	$k = 4.7 \times 10^{-12}\, (T/300)^{-1.4}\ cm^3\ s^{-1}$

[a] Reaction numbers correspond to those used in the text.
[b] From Ref. [11] unless otherwise noted.
[c] Measured in the present study.

features belong to NO and the 250 nm peak corresponds closely to the spectrum of ozone.

Whereas NO is an expected product of reaction (4), the formation of O_3 bears explanation. The relative steady state concentration of nitric oxide relative to FNO in the above chain reaction is very small, $< 2\%$ by UV absorption, but not zero. There ensues a reaction

$$HO_2 + NO \rightarrow OH + NO_2 \qquad (5)$$

that is minor in the transient experiments, but is amplified by the chain mechanism. Thus, NO_2 is present at the time of the laser pulse and is photolyzed to produce NO and oxygen atoms, the latter of which combine rapidly with O_2, owing to the latters high concentration, to form ozone. The amount of ozone observed experimentally, $(1.5–3) \times 10^{13}$ cm^{-3} is consistent with the amount expected from photolysis of the predicted steady state NO_2 level of $\approx 2 \times 10^{14}$ cm^{-3}.

An example of the HO_2 and NO concentration versus time profiles that are obtained from fits of the UV spectra is shown in Fig. 2. The data labeled 'HO_2' actually represent the composite concentration $[HO_2] + 3[FO_2]$. The latter species is formed from the competition between reaction (2) and

$$F + O_2 + M \rightarrow FO_2 + M. \qquad (6)$$

The relative concentrations of H_2 and O_2 are ordinarily adjusted to limit FO_2 formation to a few

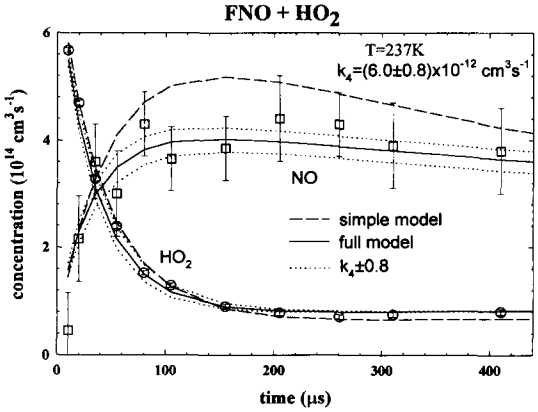

Fig. 2. Disappearance of HO_2 and appearance of NO in the reaction of FNO with HO_2. Concentrations are determined by fitting reference spectra of HO_2 and NO to the time resolved UV spectra of the reaction mixture. Error bars are the 2σ intervals for the fits and do not include $\approx 10\%$ and $\approx 20\%$ errors in the UV cross sections of HO_2 and NO, respectively. Solid lines represent best fit predictions from the reaction model of Table 1. Dotted lines show the dependence of the fit to the error bars on k_4. The dashed lines indicate the predictions of the simple model discussed in the text.

percent; yet it must be kept low enough to curtail the extent of the chain reaction. The UV spectra of HO_2 and FO_2 are sufficiently similar in shape to prevent us from assigning these species individual concentration values based on deconvolution of the spectra of the reaction mixture. Thus, the composite concentra-

Table 2
Results of rate constant measurements

Temperature (K)	Conditions					Results k_4 (10^{-12} cm^3 s^{-1})
	FNO (10^{14} cm^{-3})	H_2 (Torr)	O_2 (Torr)	P_{tot} (Torr)	$[F]_o$ (10^{14} cm^{-3})	
223	36	8.4	57	669	7.0	9.5 ± 3.0
235	15	23	41	557	6.1	5.0 ± 2.0
237	33	13	47	546	6.8	6.0 ± 0.8
255	49	7.6	59	700	7.1	5.5 ± 1.5
257	40	19	48	567	6.3	4.7 ± 0.6
273	45	7.4	60	697	6.8	4.3 ± 0.8
275	28	16	47	558	5.8	4.8 ± 0.9
294	41	16	49	576	6.1	3.2 ± 0.5
300	60	11	83	608	4.6	3.1 ± 0.7
300	84	3.2	9.6	552	3.0	2.5 ± 0.9
300	152	4	32	570	3.7	2.8 ± 1.2
325	28	15	53	600	5.7	2.8 ± 1.0
327	36	6.1	59	692	6.4	3.2 ± 0.8

tion is shown, with the factor of 3 arising from the threefold higher intensity of the FO_2 absorption [14] relative to that of HO_2.

The rate constant for the FNO + HO_2 reaction is determined by fitting the reaction model in Table 1 to the data, treating k_4 as an adjustable parameter. For the example of Fig. 2, this leads to the best fit predictions of HO_2 and NO concentration versus time profiles shown by the solid lines. A number of the reactions in Table 1, while included to enable the best determination of k_4 possible, are of rather minor importance to explain the data. The principal causes of the observed HO_2 decay are the reaction between HO_2 and FNO and the self-reaction

$$HO_2 + HO_2 \rightarrow H_2O_2 + O_2. \quad (7)$$

The predicted HO_2 decay based on these two reactions alone and using the same value for k_4 as obtained for the full model quite closely mimics the prediction from the full model. The NO rise based solely on reactions (4) and (1), shown by the dashed line, somewhat overestimates the observed concentrations. This overestimate is almost entirely eliminated upon including the reaction between HO_2 and NO.

Table 2 collects the rate constants of the FNO + HO_2 reaction measured between 223 and 327 K. The experiments are run under pseudo first order conditions; thus, noise in the concentration versus time profiles ought to contribute the largest source of error and the uncertainty in HO_2 UV cross section relatively little. The FNO concentration, however, is not straightforwardly determined and introduces an additional source of uncertainty. Nominally it would equal the NO concentration, but some is lost in the course of the chain reaction, for example, via conversion to NO_2. How much is lost depends on the total pressure, temperature, and gas composition, particularly the H_2/O_2 ratio. The FNO concentration is determined, with H_2 present, from its absorbance in the 300–320 nm region, taking into account the loss of F_2 and the formation of NO_2 by the chain mechanism. Typically the uncertainty in FNO level is in the range of $\pm$(10–20)%. The uncertainty could be lowered by decreasing the H_2/O_2 ratio, but this introduces a different problem, namely it enhances FO_2 formation. With the lower H_2/O_2 ratios there was some difficulty, particularly

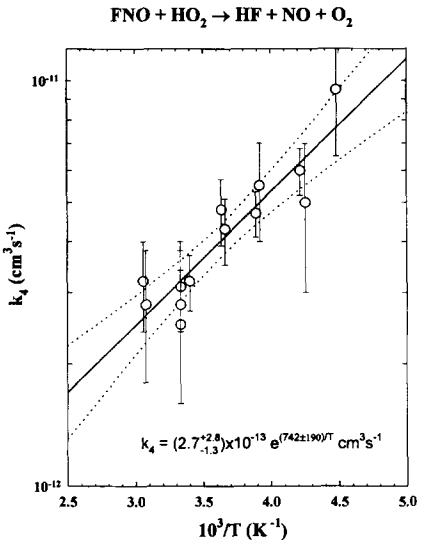

Fig. 3. Temperature dependence of the FNO + HO_2 rate constant. Error bars represent 2σ deviations from uncertainties due to noise in the concentration versus time data, initial concentration of FNO, and interference from FO_2. The solid line illustrates the fit of the rate constants to an Arhennius expression. Dotted lines indicate the 95% confidence intervals for the fit.

at reduced temperatures, in reproducing the long time $[HO_2] + 3[FO_2]$ limit. This could be corrected by increasing k_2/k_6, but at the expense of introducing an approximately 15% uncertainty into the determination of k_4. A statistical sum of the uncertainties from noise, FNO concentration, and FO_2 interference yields the reported error bars of $\pm$(15–40)%. The influence of the error bars on the model predictions is illustrated for the example in Fig. 2.

Fig. 3 illustrates the temperature dependence of the FNO + HO_2 rate constant. Note that the scatter in the data points is commensurate with the above error estimates. A best fit (weighted by the relative errors) of the rate constants to an Arhennius expression yields $k_4 = (2.7^{+2.8}_{-1.3}) \times 10^{-13} e^{(742 \pm 190)/T}$ cm^3 s^{-1}. The negative temperature dependence suggests that the reaction proceeds via a rate limiting HO_2FNO complex formation followed by rapid rearrangement of the complex into products.

Owing to interference from the chain reaction in which the FNO + HO_2 reaction participates it was not possible to extract reliably quantitative rate constants at total pressures less than about 500 Torr. However, two observations suggest that the reaction

is equally rapid at significantly lower total pressures, such as those pertinent to the stratosphere. First, rapid formation of NO was observed, though not quantified, at $P_{tot} \approx 200$ Torr. Secondly, the observed negative temperature dependence suggests that the reaction proceeds through an intermediate complex. Since 500 Torr N_2 is insufficient to collisionally stabilize this complex, it is likely that the kinetics remains unchanged as the pressure is lowered.

3.2. $FNO + CH_3O_2$

Owing to its moderately rapid reaction with HO_2, it is of interest to explore the reactivity of FNO with other peroxy radicals. From an atmospheric standpoint the methylperoxy radical serves as an important example. When CH_4 replaces H_2 in the gas mixture none of the signs of chain reaction, such as a temperature rise, are apparent. Similarly, addition of CH_4 to a gas mixture containing FNO and O_2 caused no observable changes in the FNO concentration. This leads to the conclusion that, at least under experimental conditions similar to those used in the experiments with HO_2, a chain reaction similar to the one discussed above is not operative.

UV spectra following the photolysis of a $F_2/NO/CH_4/O_2/N_2$ gas mixture at 295 K reveal a slow decay of a broad absorption feature centered at 238 nm and attributed to CH_3O_2. This decay occurs over a 5 ms timescale, far slower than the HO_2 decay in Fig. 2. Comparison of the CH_3O_2 decay in the presence versus the absence of FNO reveals the former decay to be a little faster, consistent with a rate constant of $k(FNO + CH_3O_2) < 5 \times 10^{-14}$ cm^3 s^{-1}. This value is reported as an upper limit, because we have not in detail explored the possible influences of secondary reactions; for example, the CH_3O_2 self reaction leads to HO_2 formation which can react with both CH_3O_2 and with FNO. Regardless of these considerations, the experiments show the rate constant for $FNO + CH_3O_2$ to be two orders of magnitude, or more, slower than that of the $FNO + HO_2$ reaction.

4. Atmospheric implications

The role of FNO in atmospheric chemistry has been debated recently following the suggestion of its importance by Dibble and Francisco [15]. In a series of letters to the editor Wallington et al. argue that its primary fate is rapid photolysis, whereas Dibble and Francisco counter by suggesting reactions that could feasibly compete with photolysis [16]. Our earlier investigation [8] revealed the reactions of FNO with O_3 and HCl to be too slow to be of consequence. A contribution of the reaction with $O(^3P)$ to the chemistry in the upper stratosphere could not be ruled out owing to the steep increase in its concentration with altitude.

Unlike with these species, FNO reacts moderately rapidly with HO_2, with the negative temperature dependence enhancing its effectiveness at stratospheric altitudes. Its influence on the atmospheric fluorine chemistry can be understood from consideration of the following cycle:

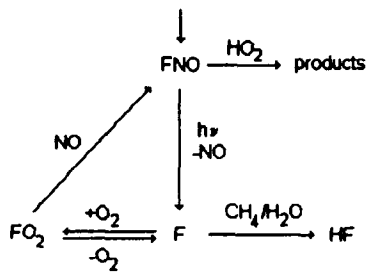

FNO formed by the reactions of CF_3O, FO_2 and FC(O)O with NO, and possibly other sources, is lost by photolysis, but reformed by the addition of O_2 to the fluorine atom photolysis product and the subsequent conversion of FO_2 to FNO. This cycle is broken by the removal of fluorine atoms via its reactions with hydrocarbons or water vapor and by the chemical or physical loss of FNO, e.g. reaction with HO_2 or uptake into water droplets.

A steady state analysis of the above cycle provides a branching ratio [8] of

$$\frac{R_{FNO}}{R_F} = \frac{k_{FNO+HO_2}[FNO]_{ss}}{k_{F+X}[F]_{ss}} = \frac{k_{FNO+HO_2}}{\Phi}\left(1 + \frac{k_{F+O_2}k_{FO_2+NO}}{k_{F+X}\left(k_{FO_2+NO} + k_{FO_2}\right)}\right)$$

for the loss of FNO relative to the loss of F atoms. Here the symbols 'k' represent pseudo first order

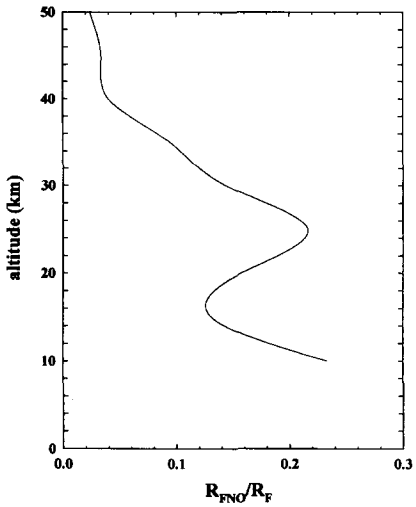

Fig. 4. Removal of fluorine from the atmosphere: variation of the ratio of FNO removed by reaction with HO_2 to F atom removal by CH_4 and H_2O as a function of altitude.

rates and X represents CH_4 and H_2O, Φ is the FNO photolysis rate, and k_{FO_2} is the FO_2 dissociation rate. This ratio is plotted as a function of altitude in Fig. 4, based on the present FNO + HO_2 rate constant, the FO_2 + NO rate constant of Li et al. [13], Hippler's [17] expression for the equilibrium between F + O_2 and FO_2, a photolysis rate [3] of 1.4×10^{-3} s^{-1}, and the atmospheric concentrations taken from Ref. [11]. R_{FNO}/R_F is sensitive to the ratio k_{FO_2}/k_{FO_2+NO}. A 10% reduction of the activation energy for FO_2 dissociation from 6711 K to the recommended value [11] of 6100 K roughly reduces R_{FNO}/R_F by a factor of 2. An increase in the FO_2 + NO rate constant would have the opposite effect.

Depending on the value of k_{FO_2}/k_{FO_2+NO}, the loss of FNO by reaction with HO_2 will constitute approximately a 10% to 20% fraction of the total removal of fluorine from the above cycle. That HO_2 reacts rapidly with FNO suggests that the reaction between OH and FNO to form HF and NO_2 might also be fast. If so, it will increase atmospheric fluorine removal via the FNO pathway. The minor difference between the two pathways is that FNO loss via reaction with HO_2 (or OH) removes peroxy radicals from the atmosphere and generates NO_x, whereas its photolysis followed by the reaction of fluorine atoms with CH_4 or H_2O creates peroxy radicals (after O_2 addition) or OH radicals, respectively. However, both pathways terminate the CFC and HCFC degradation processes, forming HF and returning the NO used in removing species such as CF_3O and FC(O)O.

[3] See comment by Wallington et al. [16].

References

[1] M.M. Maricq, J.J. Szente, T.S. Dibble and J.S. Francisco, J. Phys. Chem. 98 (1994) 12294.
[2] P. Biggs, C.E. Canosa-Mas, D.E. Shallcross, R.P. Wayne, C. Kelly and H.W. Sidebottom, Alternative Fluorocarbon Environmental Acceptability Study Workshop, March 1993, Dublin.
[3] J.S. Francisco, A.N. Goldstein, Z. Li, Y. Zhao and I.H. Williams, J. Phys. Chem. 94 (1990) 4791.
[4] O.J. Nielsen and J. Sehested, Chem. Phys. Letters 213 (1993) 433.
[5] T.J. Wallington, M.D. Hurley and W.F. Schneider, Chem. Phys. Letters 213 (1993) 442.
[6] M.M. Maricq and J.S. Szente, Chem. Phys. Letters 213 (1993) 449.
[7] A.R. Ravishankara, A.A. Turnipseed, N.R. Jensen, S. Barone, M. Mills, C.J. Howard and S. Solomon, Science 263 (1994) 71.
[8] T.J. Wallington, W.F. Schneider, J.J. Szente, M.M. Maricq, O.J. Nielsen and J. Sehested, J. Phys. Chem. 99 (1995) 984.
[9] M.M. Maricq and J.J. Szente, J. Phys. Chem. 96 (1992) 10862.
[10] M.M. Maricq and J.J. Szente, J. Phys. Chem. 98 (1994) 2078.
[11] W.B. DeMore, S.P. Sander, D.M. Golden, R.F. Hampton, M.J. Kurylo, C.J. Howard, A.R. Ravishankara, C.E. Kolb and M.J. Molina, Chemical kinetics and photophysical data for use in stratospheric modeling, JPL publication 92-20 (1992).
[12] W.G. Mallard, F. Westley, J.T. Herron, R.F. Hampson and D.H. Frizzell, NIST chemical kinetics database, version 6.0 (NIST, Gaithersburg, 1994).
[13] Z. Li, R.R. Friedl and S.P. Sander, submitted for publication.
[14] M.M. Maricq and J.J. Szente, J. Phys. Chem. 96 (1992) 4925.
[15] T.S. Dibble and J.S. Francisco, J. Phys. Chem. 98 (1994) 5010.
[16] T.J. Wallington, W.F. Schneider, O.J. Nielsen and J. Sehested, J. Phys. Chem. 98 (1994) 10373 (comment); T.S. Dibble and J.S. Francisco, J. Phys. Chem. 98 (1994) 10374 (reply).
[17] H. Hippler, private communication, 1993.